Optimizing Self-compacting Concretes with Recycled Plastic Aggregate: Fresh and Hardened Properties – Experimental Study and Modeling

Said ZAOUAI [1], Rachid RABEHI [2, 3] *, Mohamed RABEHI [3]

[1] *Laboratory of Eco-Materials: Innovations & Applications (EMIA), Civil Engineering Department, University of Djelfa, 17000, Algeria*
[2] *Faculty of Civil Engineering, University of Sciences & Technology Houari Boumediene (USTHB), Algiers, Algeria*
[3] *Civil Engineering and Sustainable Development Laboratory, University of Djelfa, Algeria*

http://doi.org/10.5755/j02.ms.38687

Received 2 October 2024; accepted 20 January 2025

This study investigates the effects of incorporating recycled polyethylene terephthalate (PET) plastic aggregate into self-compacting concrete (SCC) as a partial replacement for natural aggregate. Six SCC mixtures were prepared with plastic aggregate replacements of 0 %, 10 %, 20 %, 30 %, 40 %, and 50 % by volume. The research examines both fresh and hardened properties of the concrete. Fresh properties were evaluated using slump flow (D, T_{500}), J-ring (D, DH), V-funnel (T_V), L-box tests ($L=H_2/H_1$), and sieve stability (Π). Hardened properties, including density (ρ_{SCC}), water absorption (A_{bsi}), ultrasonic pulse velocity (V_{ult}), compressive strength (C_S), tensile strength (T_S), and dynamic modulus of elasticity (E_d), were measured at various curing ages up to 84 days. Results indicate that plastic aggregate inclusion generally improved flowability and passing ability but slightly decreased segregation resistance in the fresh state. In the hardened state, increasing plastic content led to decreased density, increased water absorption, and reduced mechanical strengths. However, mixes with up to 10 % plastic aggregate (SCC_{10}) maintained comparable performance to the control mix (SCC_0). The study also establishes a correlation between compressive strength and ultrasonic pulse velocity, providing a non-destructive method for strength estimation. It also establishes a correlation between tensile strength and ultrasonic pulse velocity. This research contributes to the development of sustainable concrete mixtures that effectively utilize plastic waste while maintaining desirable characteristics for construction applications, balancing environmental benefits with performance considerations.

Keywords: self-compacting concrete, recycled plastic aggregate, fresh state properties, hardened state properties, ultrasonic pulse velocity, sustainability, correlation.

1. INTRODUCTION

Since its development in Japan during the 1980s, self-compacting concrete (SCC) has brought about a significant transformation in the construction industry [1]. This innovative concrete has streamlined construction processes and improved the quality of concrete structures, marking a pivotal advancement in concrete technology. Its ability to flow under its own weight, fill formwork, and achieve full compaction without external vibration has led to numerous advantages, including reduced labor costs, improved durability, reduced noise, and enhanced construction speed [2]. Concurrently, there is a challenge and an opportunity to solve environmental issues posed by the building sector, which contributes nearly 40 % of global carbon emissions [3]. Concrete, the most popular building material in the world, uses a tremendous amount of natural resources, with the manufacturing of cement alone accounting for almost 8 % of global CO_2 emissions [4]. Given this, managing plastic waste and reducing the high carbon footprint of building materials are two major environmental challenges that might be addressed concurrently by using plastic waste as aggregates in concrete. The circular economy and waste valuation concepts are in line with the idea of employing plastic aggregates in concrete [5]. By reusing plastic garbage that might otherwise wind up in landfills or the ocean, this method not only lessens pollution in the environment but also preserves natural resources that are often utilized as aggregates for concrete. Research on the performance and viability of concrete using plastic aggregates has exploded in the past several years [6].

The remarkable acceleration in the pace of construction, in response to population growth and the accompanying growing demand for facilities and infrastructure, imposes significant challenges on the construction sector. This reality calls for the development of innovative strategies to diversify the sources of building materials, with the aim of preserving natural resources and improving the properties of concrete [7, 8]. Hence the use of various types of waste, such as construction debris, rubber, and plastic waste, has emerged as an ideal dual solution that contributes to reducing the environmental impact of the construction industry while addressing the problem of waste disposal. Concurrently, the global plastic waste crisis has reached alarming proportions, with an estimated 380 million tonnes of plastic waste generated annually as of 2023. The construction industry, being one of the largest consumers of raw materials, presents a unique opportunity to address both technological advancement and environmental sustainability through the innovative use of recycled

* Corresponding author: R. Rabehi
E-mail: *rachid.rabehi@usthb.dz*

materials [9, 10]. This startling statistic highlights the critical need for creative approaches to waste management and recycling of plastic materials. As early as the 1970s and 1980s, researchers explored the idea of incorporating plastic waste into concrete [11 – 13]. Initial studies focused on using plastic waste as a partial replacement for fine or coarse aggregates in concrete mixtures [14 – 17].

During the last years of the last century and up to the present time, researchers have intensified their efforts in studying types of concrete containing various types of plastic waste, including polyvinyl chloride (PVC), polypropylene (PP), and polyethylene terephthalate (PET). Concrete mixtures have used these plastic materials in varying proportions as alternatives to traditional aggregates, whether fine or coarse. These studies investigated the properties and usage of these mixtures [7, 15]. The incorporation of plastic waste as a partial replacement for fine or coarse natural aggregates in SCC represents a confluence of these two significant trends in civil engineering: the pursuit of high-performance, efficient construction materials and the urgent need for sustainable waste management solutions. Polyethylene terephthalate (PET), primarily sourced from discarded plastic bottles, stands out as a particularly promising candidate for this application due to its widespread availability and relatively consistent properties [18]. The use of plastic aggregates in SCC is motivated by several factors, including environmental impact. Utilizing plastic waste in self-compacting concrete can significantly reduce the volume of plastic ending up in landfills or oceans, contributing to circular economy principles and reducing the concrete industry's environmental footprint. Resource conservation where partial replacement of natural aggregates with plastic can help conserve natural resources, addressing concerns about the depletion of sand and gravel reserves [19]. Additionally, the lower density of plastic compared to natural aggregates offers the potential for producing lightweight concrete, which can be advantageous in certain structural applications. Also, some studies have suggested that the inclusion of plastic aggregates can improve certain concrete properties, such as thermal insulation and impact resistance [20]. However, the incorporation of plastic aggregates in SCC also presents several challenges that need to be carefully addressed, where plastic aggregates typically have lower strength and stiffness compared to natural aggregates, which can lead to reduced mechanical properties in the resulting concrete. Houcine et al. [21] found that by replacing natural gravel with plastic gravel by 15 %, the compressive strength of ordinary concrete remained acceptable and appropriate. After adding an extra 15 %, the compressive strength of ordinary concrete was reduced by half compared to the reference concrete.

The hydrophobic nature of most plastics can result in poor bonding between the plastic particles and the cement paste, potentially affecting the concrete's structural integrity [11, 22]. While plastic aggregates may enhance flowability due to their smooth surface, they can also affect the stability and segregation resistance of the SCC mix. The long-term behavior of concrete containing plastic aggregates, including potential chemical interactions and aging effects, remains a subject of ongoing research. Additionally, ensuring consistent properties of recycled plastic aggregates can be challenging due to variations in the source material. Given these potential benefits and challenges, there is a critical need for comprehensive research to quantify the effects of plastic aggregate incorporation on the fresh and hardened properties of SCC. While previous studies have explored the use of plastic waste in conventional concrete [23, 24], the unique rheological requirements of SCC necessitate a focused investigation in this context.

The current research aims to conduct a comprehensive investigation into the effects of incorporating PET plastic aggregate on SCC. To achieve this objective, natural aggregate will be partially replaced with PET plastic aggregate at increasing levels from 0 % to 50 % with a step of 10 % by volume. The study will examine both fresh and hardened properties. Fresh properties will be assessed through slump flow (D, $T500$), J-ring (D, DH), V-funnel (T_V), L-box tests ($L = H_2/H_1$), and sieve stability (Π) to evaluate flowability, passing ability, and segregation resistance. Hardened properties will be determined by measuring density (ρ_{SCC}), ultrasonic pulse velocity (V_{ult}), water absorption by capillary action (A_{bsi}), compressive strength (C_S), tensile strength (Ts), and dynamic modulus of elasticity (E_d). Additionally, this research will explore potential correlations between laboratory compressive strength results and non-destructive ultrasonic pulse velocity measurements, aiming to develop more efficient testing methods. Ultimately, this study seeks to contribute to the development of sustainable concrete mixtures that effectively utilize plastic waste while maintaining or enhancing SCC's desirable characteristics, thus improving both environmental sustainability and concrete performance in construction applications.

2. MATERIALS AND METHODS

2.1. Materials

To meet the research objectives, we utilized materials that were locally sourced. Consistent material sources were maintained across all SCC mixes throughout the experimental study.

2.1.1. Cement

In this study, Portland Cement CEM I 52.5R was the primary binder used. This high-strength cement had a specific gravity of 3.16, and its Blaine fineness was 3952 cm^2/g. Table 1 provides a comprehensive characterization of the cement used in our experiments, including its physical properties and chemical and mineralogical composition.

2.1.2. Fine aggregates

In this study, we used natural Oued sand in all self-compacting concrete mixes. This sand has a specific gravity of 2.64 g/cm^3 and a fineness modulus of 2.28. Table 2 details the comprehensive properties of the sand, and Fig. 1 depicts its grain size distribution curve, offering a comprehensive characterization of the fine aggregate we used in our experiments.

2.1.3. Coarse aggregates

In our study, crushed limestone served as the coarse aggregate component.

Table 1. Physical properties, chemical and mineralogical composition of cement used

Physical properties								
Fineness, cm^2/g	3952							
Apparent density, kg/m^3	1028							
Specific density, kg/m^3	3161							
Chemical composition, %								
CaO	SiO_2	Al_2O_3	Fe_2O_3	SO_3	MgO	Na_2O	K_2O	LOI
62.39	21.23	5.11	3.41	2.93	1.89	0.10	0.67	1.79
Mineralogical composition, %								
C_3S		C_2S		C_4AF		C_3A		
62.38		14.87		12.17		7.08		

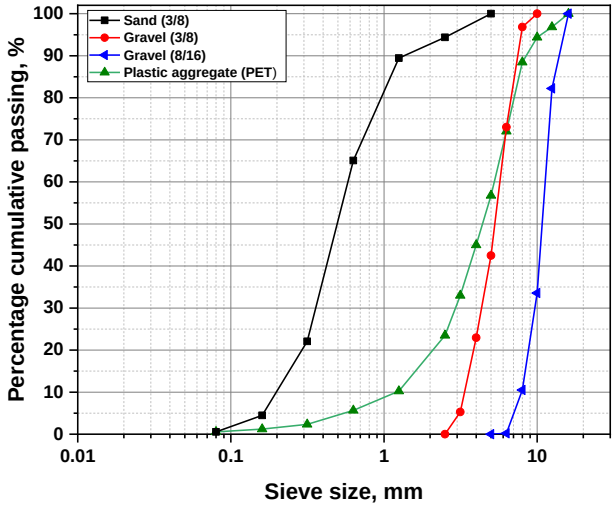

Fig. 1. Grading curves of the coarse and fine aggregates used (natural and plastic)

This material was characterized by a maximum particle size of 16 mm, a specific gravity of 2.69, and a water absorption rate of 0.52 %. To provide a comprehensive understanding of the aggregate's characteristics, we have compiled its physical and mechanical properties in Table 2. Fig. 1 displays the particle size curves of the two gravel fractions used.

2.1.4. Plastic aggregates

In this study, recycled polyethylene terephthalate is obtained from post-consumer plastic bottles. The plastic waste was cleaned, shredded, and processed to achieve particle sizes similar to the natural aggregates. The coarse plastic aggregates were graded following ASTM C330/C330M [25] and ACI E1–07 [26] using a MATEST A060–01 autosieve shaker. Fig. 2 shows the plastic materials used. The aggregate characteristics and physical properties of plastic aggregates used are presented in Table 3.

Fig. 2. Plastic aggregates used

Table 3. Physical properties of plastic aggregate (PET)

Physical property	Plastic aggregate		
	(0/5)	(3/8)	(3/16)
Specific gravity, g/cm^3	1.15	1.29	1.37
Bulk density, kg/m^3	164	539	547
Degree of absorption, %	1.35	0.38	0.41
Fineness modulus	2.40	–	–

2.1.5. Water

For mixing and curing, potable, clean water was used. As a reactant and a medium for the hydration process, water is essential to the mixing and curing of concrete. Use potable water that is devoid of dangerous contaminants, such as oils, acids, alkalies, salts, organic compounds, or other chemicals that might affect reinforcement or concrete, for the best possible quality of concrete. A key component in determining the ultimate product's strength and longevity is the water-to-cement ratio; concrete with lower ratios is often stronger. A sequence of chemical processes that bind the aggregate components together are started when water is added to the cement during mixing.

Table 2. Physical-mechanical properties of the fine and coarse aggregates used

Components	Property of SCC			
	Apparent density mass	Absolute density mass	Degree of absorption	Los Angeles coefficient
	g/cm^3	g/cm^3	%	%
Sand (0/5)	1.546	2.637	1.34	–
Gravel (8/16)	1.367	2.687	2.10	24.30
Gravel (3/8)	1.347	2.691	2.20	22.90

2.2. Preparation of plastic aggregates

- Sorting and cleaning: plastic waste was manually sorted to remove contaminants and washed with water.
- Shredding: a mechanical shredder was used to reduce the plastic to sizes ranging from 0.1 to 16 mm.
- Grading: shredded plastic was sieved to match the gradation of the natural aggregates being replaced.

The plastic blocks after crushing the PET bottles were in the form of flat, irregular flakes, characterized by their irregular geometric patterns, flat structure, sharp and angular edges, and ranging from approximately rectangular to completely asymmetrical shapes, with varying length-to-width ratios.

2.3. Formulation of self-compacting concrete

The creation of SCC demands a departure from traditional methods such as Dreux-Gorisse, which are suitable only for regular concrete [27, 28]. In the realm of SCC, formulation is predominantly guided by empirical approaches, drawing upon the wealth of knowledge accumulated in recent years.

The process of developing SCC mixtures is a delicate balancing act. It begins with carefully crafted initial compositions, often inspired by specialized literature. These serve as a foundation, which is then refined through a series of precise adjustments. Particular attention is paid to critical ratios such as water-to-cement (W/C) and superplasticizer-to-cement (Sp/C). These ratios are fine-tuned based on the performance of mortar tests, with the goal of achieving optimal spread without compromising the mixture's integrity through segregation or bleeding.

In our pursuit of excellence, we formulated a reference SCC_0 using 100 % crushed limestone gravel, eschewing plastic aggregates entirely. This composition was meticulously engineered to meet the exacting standards of self-placing concrete, embodying the perfect fusion of flowability and stability that defines superior SCC.

The selection of component ratios in 1 m^3 of concrete must be based on the characteristics provided [29]. In concrete mix design, the total volume of components equals 1000 liters, comprising cement (C), sand (S), natural gravel (NG), plastic aggregates (PA), water (W), and air (A). The ratio of gravel to sand is approximately 1:1, ensuring a balanced aggregate distribution. The mix includes 1.3 % of a specific admixture (Sp), enhance properties of the concrete in fresh state. The W/C is 0.40. The cement content is specified at 450 kg per cubic meter, which is relatively high and suggests a high-strength concrete mix. This composition aims to achieve a specific set of properties in the fresh and hardened states of the concrete.

Six SCC mixtures were prepared with plastic aggregate replacements of 0 %, 10 %, 20 %, 30 %, 40 %, and 50 % by volume of plastic aggregates. Table 4 lists the abbreviations used in our research for the various SCCs tested.

The compositions of these various concrete mixtures are summarized in Table 5, providing a comprehensive overview of the formulations used. These SCC mixtures were formulated in accordance with the latest EFNARC guidelines [30].

Table 4. The abbreviations for all SCCs

Notations	Designations
SCC_0	SCC with 0 % (PA) and 100 % (NA)
SCC_{10}	SCC with 10 % (PA) and 90 % (NA)
SCC_{20}	SCC with 20 % (PA) and 80 % (NA)
SCC_{30}	SCC with 30 % (PA) and 70 % (NA)
SCC_{40}	SCC with 40 % (PA) and 60 % (NA)
SCC_{50}	SCC with 50 % (PA) and 50 % (NA)
NA – natural aggregates	

2.4. Mixing procedure and curing

The concrete mixing process begins with dry mixing of coarse aggregates and half of the fine aggregates for 30 seconds. Next, cement and supplementary cementitious materials are added and mixed for another 30 seconds. Then, 70 % of the total water is introduced and mixed for 1 minute. Pre-weighed plastic aggregates are added and mixed for 30 seconds. The superplasticizer, combined with the remaining 30 % of water, is slowly added while mixing continues. This is followed by a main mixing period of 3 minutes. The mixture is then allowed to rest for 2 minutes before a final mixing phase of 2 minutes completes the process.

After mixing, the formulations for the studied concretes were created using cube-shaped molds measuring $15 \times 15 \times 15$ cm^3. The following procedures were then carried out: The concrete specimens were subjected to open-air curing by being left exposed to laboratory conditions (relative humidity of 45 ± 2 % and temperature of 21 ± 2 °C) for periods of 7, 28, 56, and 84 days. Additionally, a separate set of samples underwent water curing for a period of 28 days. These diverse curing methods were employed to comprehensively assess the concrete's properties under different environmental conditions and time frames, allowing for a thorough evaluation of the material's performance and characteristics.

Table 5. Composition of all SCC in kg/1m^3

Mix	Compositions of SCC						
	Cement	Water	Sand	Gravel	Plastic	SP	W/C
SCC_0	450	180	890.30	880.60	0	1.3	0.40
SCC_{10}	450	180	845.79	836.57	32	1.3	0.40
SCC_{20}	450	180	801.28	792.54	64	1.3	0.40
SCC_{30}	450	180	756.76	748.51	96	1.3	0.40
SCC_{40}	450	180	712.25	704.48	128	1.3	0.40
SCC_{50}	450	180	667.73	660.45	160	1.3	0.40

2.5. Testing methods

2.5.1. Fresh properties

The fresh properties of the SCC mixtures were evaluated using a comprehensive suite of tests in accordance with EFNARC guidelines [28]. The slump flow test was conducted to assess the flowability and filling ability of the SCC, measuring both the final spread diameter (D) and the time taken to reach a 500 mm spread (T_{500}). The J-ring test was performed to evaluate the passing ability of the SCC through reinforcement, while the V-funnel test provided insights into the viscosity and filling ability of the mixtures. The L-box test was utilized to assess the passing ability and flowability of SCC in confined spaces, with the ratio of heights at both ends of the box (H_2/H_1) being recorded. Finally, the sieve segregation resistance test was carried out to determine the resistance of the SCC mixtures to segregation. Fig. 3 shows all tests performed in a fresh state.

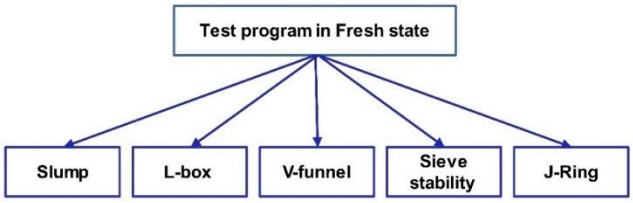

Fig. 3. Tests performed in a fresh state

2.5.2. Hardened properties

A series of standardized tests, conducted at various ages, thoroughly evaluated the hardened properties of the concrete specimens. The density of concrete containing different proportions of plastic aggregate was measured after 28 days. Compressive strength tests were conducted at 7, 28, 56, and 84 days to evaluate the strength development over time and the long-term strength characteristics of the mixtures. The mechanical and durability properties were also evaluated at 28, 56, and 84 days. Tensile strength was assessed using three-point bending tests, providing insights into the material's resistance to tensile forces. Water absorption tests were performed to evaluate the porosity and durability aspects of the hardened concrete, offering valuable information about its resistance to water penetration. Furthermore, ultrasonic pulse velocity measurements were taken on the same samples before conducting compressive resistance experiments, serving as a non-destructive method to assess the concrete's internal structure and homogeneity. Also, the dynamic modulus of elasticity was measured. This extensive battery of tests yielded a holistic understanding of the mechanical properties, durability characteristics, and internal quality of the hardened concrete specimens. The results provide a comprehensive overview of the behavior of (SCC) incorporating different percentages of plastic aggregate, allowing for a thorough evaluation of how this inclusion affects the concrete's performance over time. Fig. 4 shows all tests performed in a hardened state.

2.5.3. Test of density

Density testing of hardened self-compacting concrete is an essential procedure for evaluating the physical properties of concrete after it has been set.

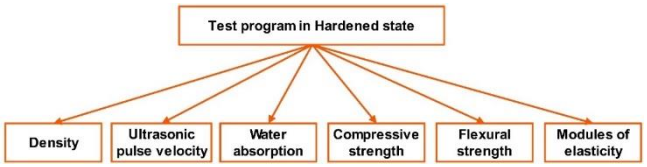

Fig. 4. Tests performed in a hardened state

This test makes it possible to determine the density of hardened concrete, a crucial parameter that directly influences its mechanical performance and durability. We conduct the measurement on cubic samples ($10 \times 10 \times 10$ cm) that have aged for at least 28 days. We weigh the sample (M_{sample}) and determine its precise volume (V_{sample}), either by geometric calculation or by water displacement. Then, using Eq. 1, we calculate density by dividing mass by volume.

$$\rho_{(SCC)} = d_{(sample)} = \frac{M_{(sample)}}{V_{(sample)}}. \quad (1)$$

2.5.4. Absorption of water testing

The water absorption test, specifically focusing on initial absorption by capillarity, evaluates the movement of liquid through concrete's porous structure due to capillary forces. This test is crucial for assessing the open porosity and porous networks within the no-slump concrete, which directly influences its water absorption characteristics.

When exposed to water without pressure, the procedure aims to measure the rate at which concrete test specimens absorb water through capillary suction. We take measurements at 28, 56, and 84 days. We dry the samples in an oven at approximately 105 ± 2 °C until they reach a constant mass before testing.

On the testing day, weigh the specimens before and after a one-hour water exposure. Next, we calculate the absorption coefficient (A_{bsi}) using the following equation:

$$A_{bsi} = \frac{M_{P2} - M_{P1}}{S_{ur} \cdot \sqrt{t}}, \quad (2)$$

where M_{P2} and M_{P1} are the test piece's mass after and before water absorption, respectively; S_{ur} is the surface area of the specimen's base 225 cm^2; t is the time duration is one hour.

This test provides valuable insights into the concrete's capillary absorption properties, which are indicative of its durability and potential resistance to water ingress.

The quantity of water absorbed per unit area within one hour of exposure can be used to deduce the size of the largest pores in the SCC sample [31, 32]. These larger capillaries are the most efficient in terms of water absorption.

To ensure accurate measurements, the side faces of the test specimens are sealed with an adhesive ribbon plastic, or any other insulating material to prevent water absorption and evaporation from the sides. This waterproofing measure prevents water evaporation from the sides and forces water movement in a uniaxial direction through the sample. The absorbed water mass is determined through successive weighings of the test tubes throughout the experiment, as illustrated in Fig. 5.

Open porosity, marked with the symbol ε, measures the relationship between unfilled spaces (void volume V_{void}) and the complete volume of material (V_{total}). This property helps determine the link between the quantity of absorbed water

per surface unit ($\Delta m/A$) and the upward distance covered by the liquid front ($H_{frontal}$).

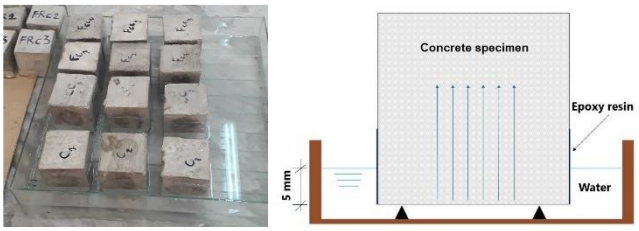

Fig. 5. Capillary water absorption test

Where it is calculated by Eq. 3:

$$\varepsilon(\%) = \left(\frac{V_{Void}}{V_{Total}}\right).100\% = \left(\frac{\left(\frac{\Delta m}{A}\right)}{\rho_w \cdot H_{frontal}}\right).100\%, \qquad (3)$$

where ε is the open porosity, expressed as a percentage; $\Delta m/A$ is the water absorption rate per surface area, measured in kilograms per square meter per square root hour; ρ_{wa} is the density of water, equivalent to 1 gram per cubic centimeter or 1000 kilograms per cubic meter; $H_{frontal}$ is the height reached by water through capillary action, set at 4 centimeters.

2.5.5. Uniaxial compression testing

The compression test is performed following the NF P 18-406 standard requirements. This process involves applying an axial compressive force to crush the SCC test cube. The load is applied continuously until the cube fails (see Fig. 6).

Fig. 6. Test specimens prior to compression testing

2.5.6. Tensile strength (three-point bending) testing

The tensile strength assessment involves rectangular prism specimens measuring 7 cm by 7 cm by 28 cm. These samples are placed on two supports and subjected to gradually increasing force until fracture occurs. The load is applied using a computerized press with a digital readout, which is programmed to increase the force at a rate of 50 N/s.

This integrated system not only controls the loading process but also records the ultimate breaking force of each specimen. The tensile strength is then determined by performing a straightforward calculation using the measured breaking force and the specimen dimensions (see Fig. 7).

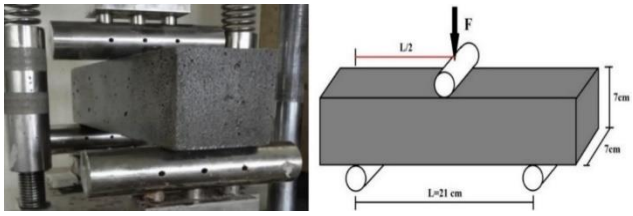

Fig. 7. Schematic and apparatus for tensile by three-point bending test

2.5.7. Effect of plastic aggregate on ultrasonic pulse velocity

Fig. 8 illustrates the apparatus used for conducting ultrasonic pulse velocity (UPV) measurements, a non-destructive evaluation technique outlined in ASTM C597-02 [33]. This test was performed on the concrete specimens immediately prior to water absorption and compressive strength assessments. To optimize signal transmission, a thin layer of coupling agent was applied to two opposite faces of the cubic samples, effectively eliminating air pockets between the concrete surface and the transducers. The transducers were then positioned on these prepared surfaces to obtain UPV readings. The ultrasonic wave propagation speed through a solid medium is a function of its density and elastic modulus, as established in acoustic theory [34]. By measuring the time taken for the ultrasonic pulse to traverse the concrete, can gain valuable insights into the concrete's internal structure and properties without causing damage to the specimen.

Fig. 8. Apparatus used for ultrasonic pulse velocity

2.5.8. Modulus of elasticity

The modulus of elasticity (E_d) test is a crucial assessment for characterizing the mechanical properties of concrete. This test measures the concrete's ability to deform elastically under applied stress, providing valuable insights into its structural performance. For self-compacting concrete, the modulus of elasticity is particularly important due to the material's unique flow characteristics and mix design. Accurate determination of E_d for SCC is essential for predicting structural behavior, assessing long-term performance, and optimizing mix designs for specific applications. The modulus of elasticity of concrete mixes was calculated using Eq. 4 [35].

$$E_{d(SCC)}(\text{GPa}) = \frac{(V_{Ult}^2(\text{km/s})^2 * \rho_{SCC}(\text{kg/m}^3))}{g*10^{+2}(\text{m/s}^2)}, \quad (4)$$

with $E_{d(SCC)}$ is the modulus of elasticity; V_{ult} is the propagation velocity of ultrasonic waves; g is the equal to 9.81 m/s², where g stands for gravitational acceleration; ρ_{SCC} is the SCC's real density.

3. RESULTS AND DISCUSSION

3.1. Fresh state properties

The properties obtained for the several self-compacting concretes tested in their fresh condition are reported in Table 6. Fig. 9, Fig. 10, and Fig. 11 also display the results.

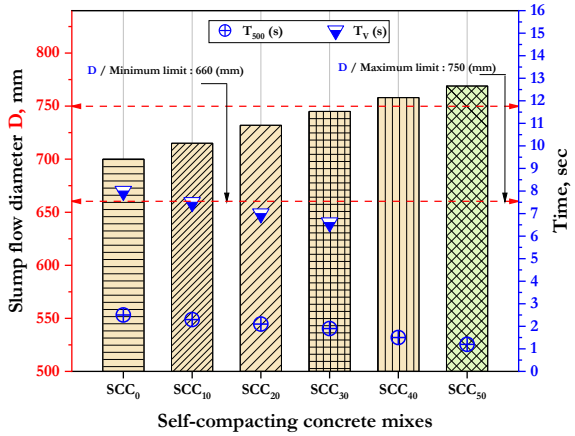

Fig. 9. Slump flow diameter, T500, and T_V of SCC mixes

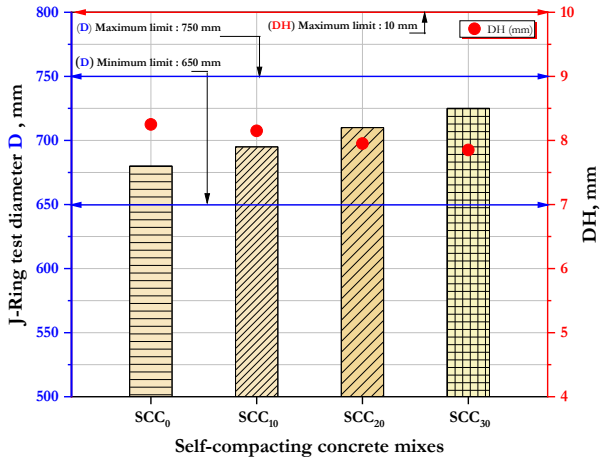

Fig. 10. J-ring diameter and DH of SCC mixes

All fresh-state features of the SCC are satisfactory and within the acceptable range, except for SCC40 and SCC50, which exhibited non-compliant slump flow test results according to SCC standards. These two mixes demonstrated flow values exceeding 750 mm, falling outside the suitable range for SCC as defined by [30], which specifies an average diameter between 660 and 750 mm.

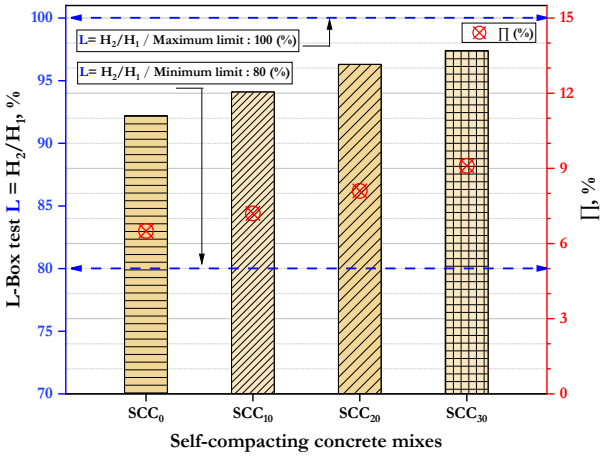

Fig. 11. L-box and segregation of SCC mixes

This indicates that the SCC_{40} and SCC_{50} mixes have excessive flowability, potentially impacting their performance and classification as self-compacting concrete. The incorporation of plastic aggregates generally improved the flowability and passing ability of SCC, as evidenced by increased slump flow and J-ring flow values, and decreased T_{500} and V-funnel times (T_V).

This result is in agreement with earlier research [36 – 38]. This can be attributed to the lower specific gravity and smoother surface texture of plastic particles compared to natural gravel. However, the segregation resistance slightly decreased with increasing plastic content, necessitating careful mix design.

A visual evaluation of all self-compacting concrete samples revealed positive results, with the exception of SCC_{50}, which showed a weakly developing milt around the edges of the concrete.

These tests collectively provided a comprehensive assessment of the key rheological properties of SCC, including flowability, filling ability, passing ability, and segregation resistance, crucial for ensuring proper performance in various applications.

3.2. Hardened state properties

3.2.1. Test of Density

Fig. 12 presents the results of our density measurements for each SCC mixture with a standard deviation. These values represent the average density calculated from three individual test pieces for each SCC formulation, ensuring a more reliable and representative result.

Table 6. Test results summary for all solid catalyst carriers in fresh state

Mix	Slump flow		J-Ring flow		L-box	V-funnel	Segregation
	D, mm	T_{500}, s	D, mm	DH, mm	L, %	T_V, s	II, %
SCC_0	700	2.5	680	8.25	92.2	8.0	6.5
SCC_{10}	715	2.3	695	8.15	94.1	7.5	7.2
SCC_{20}	732	2.1	710	7.95	96.3	7.0	8.1
SCC_{30}	745	1.9	725	7.85	97.4	6.6	9.1
SCC_{40}	758	1.5	-	-	-	-	-
SCC_{50}	768	1.2	-	-	-	-	-

This approach of using multiple samples helps to minimize the impact of potential variations or anomalies in individual specimens, providing a more accurate overall assessment of each concrete mixture's density characteristics.

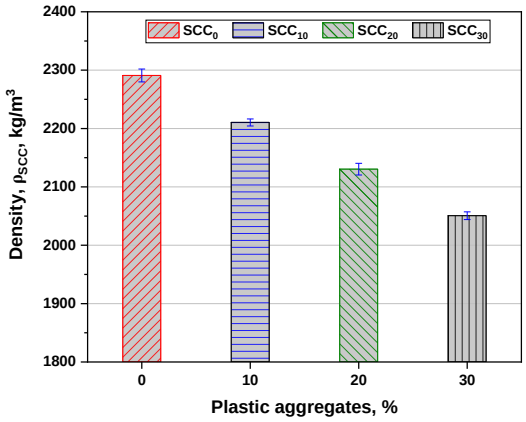

Fig. 12. Effect of plastic aggregate on apparent density

According to the results shown in Fig. 12, the density of SCC Control without plastic aggregate SCC_0 (0 % plastic aggregate) is 2290.85 kg/m³. With 10 % plastic aggregate replacement SCC_{10}, we observe a decrease in density to approximately 2210.40 kg/m³. At 20 % replacement SCC_{20}, the density further decreases to about 2130.30 kg/m³, and with 30 % plastic aggregate SCC_{30}, the density is around 2050.60 kg/m³. These results demonstrate a clear inverse relationship between the percentage of plastic aggregate and the density of the SCC mixture. These results are logical and consistent with previous research [37, 38].

The density decreases with increasing plastic aggregate content, attributed to factors such as plastic aggregates have a lower density than natural aggregates, void content, water absorption, and bonding characteristics. Plastic has a lower density compared to traditional natural aggregates, which reduces the mixture's density. The different shape and surface texture of plastic aggregate may affect packing density and increase void content in the concrete matrix [39].

3.2.2. Absorption of water testing

The initial water absorption coefficients (A_{bsi}), measured in kg·m^{-2}·h$^{-1/2}$ after one hour of exposure, are presented for all tested self-compacting concrete (SCC) mixtures in Table 7 and Fig. 13. These coefficients quantify the capillary absorption rate, expressing the data as a rate of gain across various SCC formulations.

Then, using Eq. 5, calculate the rate of gain:

$$A_{bsi} = \left| \frac{A_{bsi_{j\,(without\ cure)}} - A_{bsi_{j\,(cure)}}}{A_{bsi_{j\,(without\ cure)}}} \right|. \quad (5)$$

Fig. 13 a illustrates that for all SCC mixes, the absorption decreases with age (28, 56, and 84 days). This trend is attributed to the long-term hydration of cement, which reduces the number and size of pores in the concrete, thereby lowering water absorption over time. The results show that plastic aggregate content impacts water absorption. The absorption values stabilize when 10 % of plastic gravel partially replaces natural gravel.

Table 7. Initial water absorption coefficients and relative gain rates for all SCC

Age in days	SCC mixtures, MPa				
	Curing	SCC_0	SCC_{10}	SCC_{20}	SCC_{30}
28	in water	1.52	1.51	1.59	1.72
	in air	2.21	2.2	2.33	2.53
	R_{Absi}	31.22	31.36	31.76	32.02
56	in water	1.47	1.37	1.53	1.69
	in air	2.17	2.15	2.29	2.51
	R_{Absi}	32.26	36.28	33.19	32.67
84	in water	1.4	1.34	1.51	1.66
	in air	2.15	2.12	2.28	2.48
	R_{Absi}	34.88	36.79	33.77	33.06

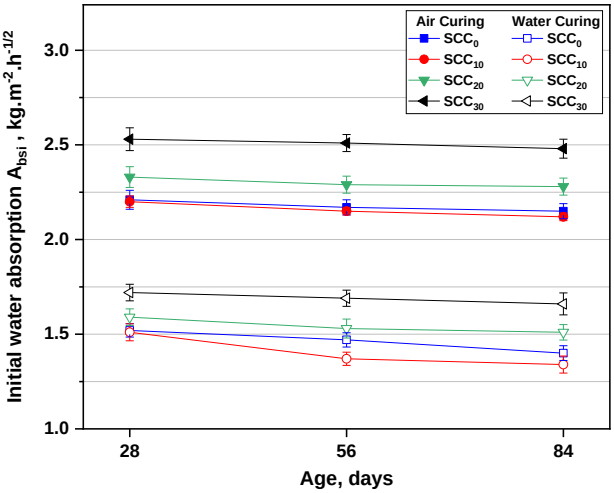

a

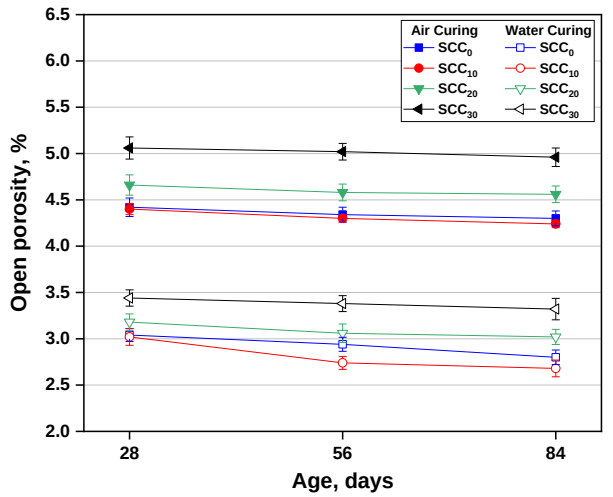

b

Fig. 13. Results for self-compacting concrete mixtures a – initial water absorption rate; b – open porosity

However, as the percentage of plastic aggregate increases beyond this point, the absorption values significantly rise compared to the reference mixture containing only natural aggregates.

The significant increase in water absorption values as the percentage of plastic aggregate exceeds 10% can be attributed to several factors. Primarily, the addition of plastic aggregate increases the concrete's overall porosity, leading to higher sorptivity. The hydrophobic nature of

plastic creates localized areas of excess water that, upon evaporation, leave behind additional pores. Poor adhesion between plastic and cement paste forms a weak interfacial transition zone, creating microcracks and pathways for water ingress. Furthermore, the irregular shape and size of plastic aggregates disrupt the concrete's homogeneity and impede proper compaction, further increasing porosity. Lastly, replacing natural aggregates with plastic reduces the overall volume of cement paste in the mixture, potentially leading to increased porosity. These combined factors explain the significant rise in water absorption values in plastic aggregate-enhanced concrete compared to the reference mixture with only natural aggregates.

At 84 days, the absorption rate of SCC with 20 % plastic (SCC_{20}) during water curing matches that of the control concrete (SCC_0) at 28 days. However, when the plastic aggregate replacement rises to 20 % and 30 %, adverse effects emerge, leading to increased porosity and compromised transport characteristics. Incorporating plastic aggregate elevates concrete porosity, resulting in higher sorptivity measurements compared to the control. The hydrophobic nature of plastic fosters localized water accumulation, which, upon evaporation, generates additional voids. Insufficient adhesion between plastic and cement paste produces a weak interfacial transition zone, causing microcracks and creating pathways for water infiltration. Furthermore, the irregular shape and varying sizes of plastic aggregates disrupt the material's uniformity and hinder effective compaction, exacerbating porosity.

The observed increase in porosity and decline in transport properties at elevated plastic aggregate levels (20 % and 30 %) stems from multiple factors. Primarily, the hydrophobic nature of plastic leads to localized water accumulation, which results in additional voids upon evaporation, thus elevating overall porosity [40 – 43]. Additionally, poor adhesion between the plastic and cement paste generates a weak interfacial transition zone, facilitating microcracks and water ingress pathways [41, 44]. This weak bond promotes water penetration into the concrete matrix. Finally, the irregular shapes and sizes of plastic aggregates disturb the material's homogeneity and hinder adequate compaction, further elevating porosity [42, 44]. These interconnected issues underscore the critical need to judiciously assess the ratio of plastic aggregates in self-compacting concrete formulations to preserve desirable performance attributes.

The Fig. 13 b demonstrates the relationship between age and open porosity percentage across different concrete mixtures over time. The results reveal that concrete specimens containing plastic aggregates consistently show higher open porosity values compared to those without plastic aggregates throughout the testing period. The data points follow a pattern where porosity generally decreases with age, but maintains clear separation between different mixture types. The lower open porosity values in specimens without plastic aggregates indicate better pore structure development. When examining the effect of water curing versus air curing, the specimens cured in water exhibited reduced open porosity levels, which can be attributed to more complete hydration reactions forming denser concrete microstructure.

3.2.3. Uniaxial compression testing

Table 8 and Fig. 14 present the average results and standard deviations from the direct compressive strength (C_{Sj}) tests conducted at 7, 28, 56, and 84 days of curing. The data in Fig. 14 clearly shows an increasing trend in compressive strength with age for the various SCC mixes. It can be observed that SCC_0 and SCC_{10} exhibited higher compressive strengths compared to SCC_{20} and SCC_{30}. These differences in strength can be attributed to the type and proportion of aggregates used in each mix, which influenced the compressive strength development through decreased or increased rates of strength gain.

Table 8. Compressive strength of all self-consolidating concrete

Age in days	SCC Mixtures, MPa				
	Curing	SCC_0	SCC_{10}	SCC_{20}	SCC_{30}
28	in water	42.90	43.50	36.90	32.04
	in air	41.50	41.45	34.70	30.50
	R_{Absi}	3.26	4.71	5.96	4.81
56	in water	46.40	48.95	37.65	32.35
	in air	43.05	43.65	35.10	32.10
	R_{Absi}	7.22	10.83	6.77	0.77
84	in water	49.80	51.75	42.10	35.35
	in air	45.50	47.85	39.20	33.70
	R_{Absi}	8.63	7.54	6.89	4.67

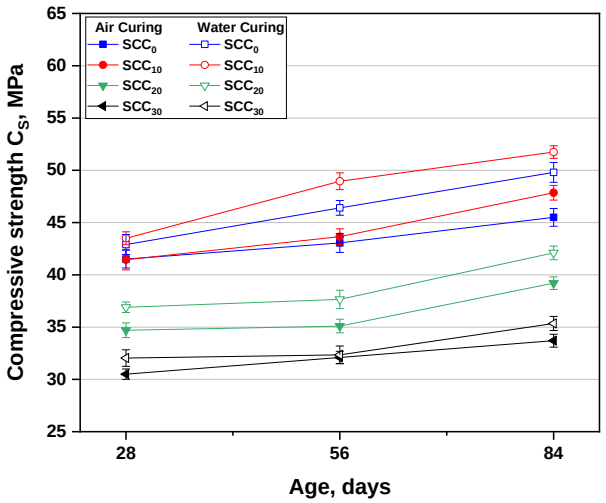

Fig. 14. Compressive strength evolution of concretes at different ages

Based on the results presented, we can observe clear trends in the properties of self-compacting concrete (SCC) with increasing plastic aggregate content. When cured in air, the compressive strength results from Fig. 15 a show a slight decrease when replacing 10 % of natural aggregate with plastic aggregate, but they decrease more significantly with higher plastic aggregate content. The results show decreases of 0.1 %, 14.3 %, and 23.7 % at 28 days for 10 %, 20 %, and 30 % replacements, respectively. The overall reduction in compressive strengths with plastic aggregate incorporation can be attributed to the lower stiffness and poorer bonding characteristics of plastic compared to natural aggregates. This explanation is supported by microscopic analyses conducted by Sharma and Bansal [45], who observed weaker interfacial transition zones between plastic aggregates and cement paste.

Other researchers Saikia et De Brito [46] also attributed the decrease in strength to softer PET particles acting as voids in the cement matrix. Additionally, the PET particles have increased porosity and wider interfacial transition zones. Also, there is poor bonding between cement paste and PET compared to natural aggregates.

In the case of curing in water (Fig. 15 b), the results were consistent with the results of curing in air, with decreases in the values being 11 % and 20 % at 28 days for 20 % and 30 % replacements, respectively. There was a slight difference when adding 10 %, where there was a slight increase in compressive strength values by 1 %, demonstrating the benefit of curing in water.

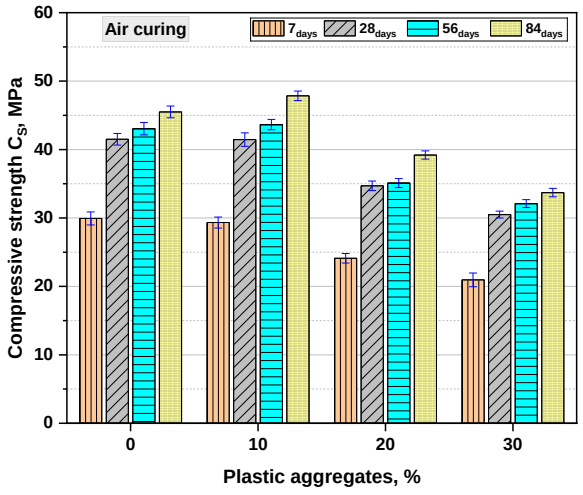

a

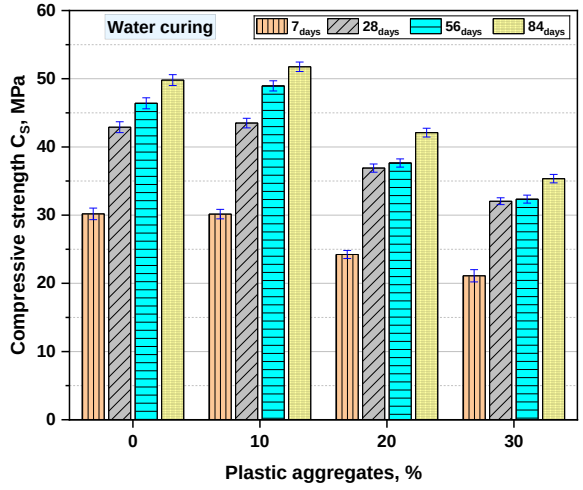

b

Fig. 15. Effects of plastic aggregates on the compressive strength of all SCC: a – under air; b – under water curing conditions

3.2.4. Tensile strength (three-point bending) testing

Fig. 16 summarizes the tensile strength values derived from three-point bending tests at 28, 56, and 84 days.

The results shown in Fig. 16 demonstrate the effects of plastic aggregate content and curing conditions on the tensile strength of SCC over time. The tensile strength development for different SCC mixtures under air curing and water curing conditions is shown for days 28, 56, and 84.

The tensile strength remains relatively stable when replacing 10 % of natural gravel with plastic aggregate. This is evident in Fig. 17, where the tensile strength for the SCC with 0 % and 10 % plastic aggregate is similar in value across all curing durations. However, there is a noticeable decline in tensile strength as the plastic content increases to 20 % and 30 %. The reduction in tensile strength for the 30 % replacement mix (SCC_{30}) compared to the control (SCC_0) is significant. This decrease in strength is likely due to the weaker bond between plastic particles and the cement matrix [47].

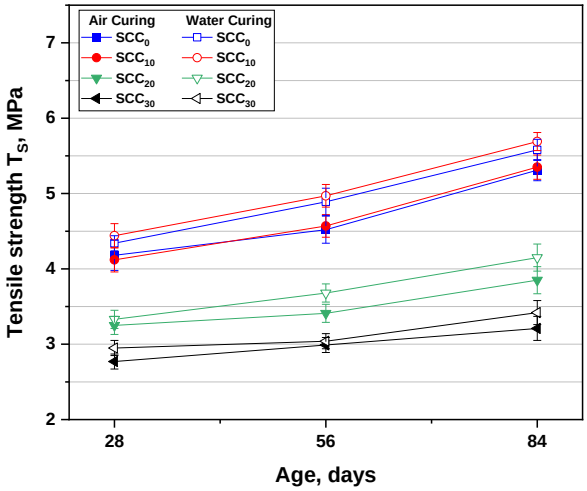

Fig. 16. Tensile strength results

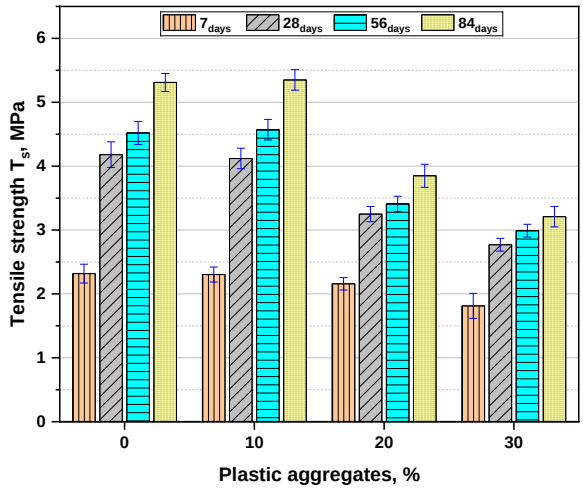

Fig. 17. Effects of plastic aggregates on the tensile strength of all SCC

3.2.5. Effect of plastic aggregate on ultrasonic pulse velocity

Fig. 18 displays experimental results showing the relationship between plastic aggregate content and UPV in SCC tested at 28, 56, and 84 days of curing. The UPV, measured in m/s, exhibits a non-linear response to increasing plastic aggregate percentages (0 %, 10 %, 20 %, and 30 %). There is a clear inverse relationship between plastic aggregate content and UPV in SCC, with UPV decreasing proportionally as plastic aggregate replacement increases, similar to the trend observed in compressive strength tests.

Initially, all three age groups show a slight increase in UPV from 0 % to 10 % plastic aggregate content, with the 84-day samples demonstrating the highest overall velocities. This initial rise suggests a potential beneficial effect of low plastic aggregate incorporation.

After the percentage of natural aggregate replaced by plastic aggregate exceeds 10 %, a significant and continuous decrease in UPV is observed across all ages with each increase in the percentage of plastic aggregate. The most severe decrease occurs when 30 % of natural aggregate is replaced by plastic aggregate (SCC30). The 84-day samples consistently maintain higher UPV values throughout the range, followed by the 56-day and 28-day samples, indicating ongoing material property development with age. Additionally, the results show an increase in pulse speed in samples treated in water compared to those treated in air.

Despite the UPV reduction, all SCC mixtures maintained good quality standards according to IS 13311-1 guidelines. These results indicate that improving curing conditions and duration can partially compensate for the lower UPV resulting from the inclusion of plastic aggregate. This enhancement may increase the feasibility of using plastic aggregate in SCC, opening new possibilities for sustainable concrete production without compromising basic physical properties. For instance, SCC with 20 % plastic aggregate (SCC_{20}) achieved a UPV of 4790.98 m/s after 84-days of water curing, outperforming the 28-day UPV for both regular SCC (SCC0) and SCC with 10 % plastic aggregate (SCC_{10}) cured in the air at speeds of 4721.04 m/s and 4728.47 m/s, respectively.

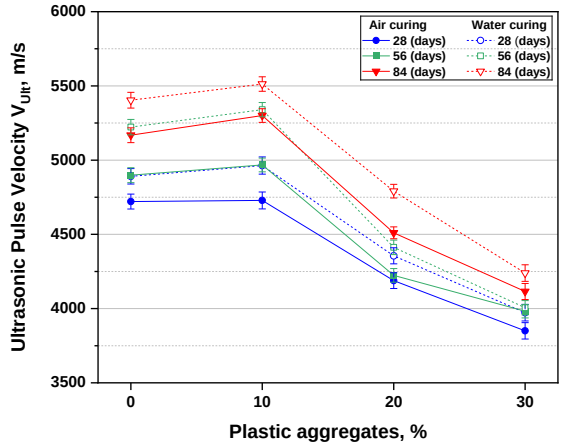

Fig. 18. Effects of plastic aggregate content on ultrasonic pulse velocity (UPV) for air-cured and water-cured SCC at 28, 56, and 84 days

3.2.6. Modulus of elasticity

The dynamic modulus of elasticity for various self-compacting concrete mixtures with varying percentages of plastic aggregates is illustrated in Fig. 19 a and b. These graphs present E_d values across different curing durations, comparing specimens subjected to air curing versus water curing conditions.

The E_d generally decreases as the percentage of plastic aggregates increases, for both air and water curing conditions. This trend is consistent across all ages (28, 56, and 84-days). For example, in air-cured samples at 84-days, E_d decreases from about 62.37 GPa at 0 % plastic aggregates (SCC_0) to approximately 35.40 GPa at 30 % plastic aggregates (SCC_{30}). Similarly, for water-cured samples at 84-days, E_d decreases from about 68.19 GPa at 0 % (SCC_0) to roughly 37.57 GPa at 30 % plastic aggregates (SCC_{30}).

The observed decrease in E_d with increasing plastic aggregate content aligns with findings from other researchers. For instance, Saikia and de Brito [46] reported a similar trend in their study on concrete with PET plastic waste aggregates. They found that the E_d decreased by up to 50 % when 30 % of natural aggregates were replaced with plastic [46].

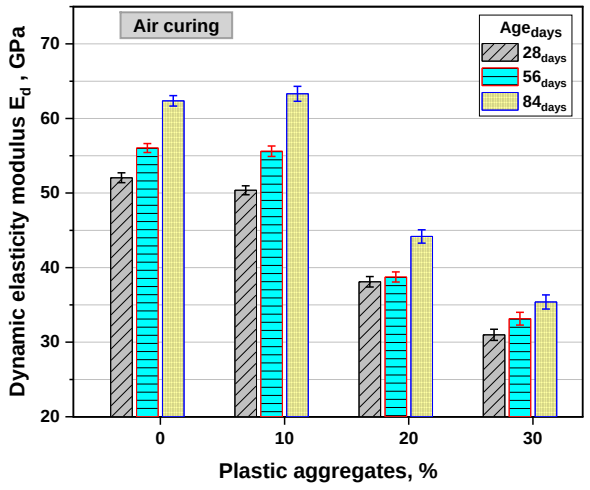

a

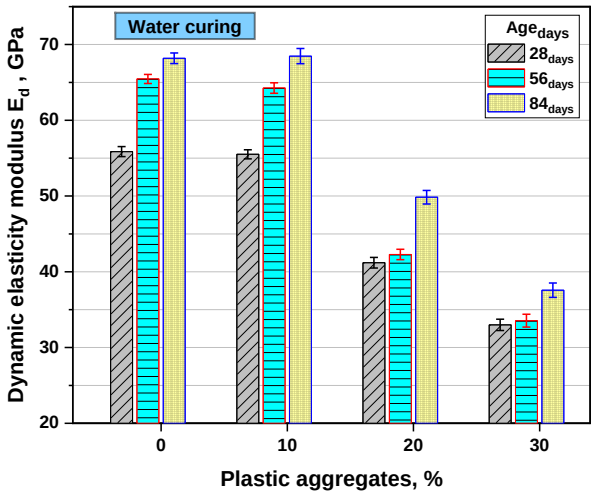

b

Fig. 19. Effects of plastic aggregate on the dynamic elasticity module: a – air curing; b – water curing

In self-compacting concrete, Jaskowska-Lemańska et al. [48] found that the addition of PET plastic aggregates resulted in a decrease in the elastic modulus ranging from 5.0 % to 32.7 %, depending on the replacement ratio, which was between 5 % and 20 %.

The dynamic modulus of elasticity increases with age for all mixtures, regardless of curing condition. This indicates continued strength development over time. For instance, in air-cured samples with 0 % plastic aggregates (SCC_0), E_d increases from about 52 GPa at 28-days to 62.37 GPa at 84-days. Water-cured samples show a similar

trend, with E_d increasing from approximately 55.86 GPa at 28-days to 68.20 GPa at 84-days for 0 % plastic aggregates.

Water curing consistently results in higher E_d values compared to air curing across all percentages of plastic aggregates and ages. This suggests that water curing is more effective in promoting strength development.

The difference is particularly noticeable at earlier ages and for mixtures with higher percentages of plastic aggregates. For example, at 28-days with 30 % plastic aggregates, water-cured samples have an E_d of about 33 GPa, while air-cured samples have an E_d of approximately 31 GPa. This is consistent with what Gu and Ozbakkaloglu [49] observed in their review of concrete with plastic materials.

The rate of increase in E_d with age is more pronounced in mixtures with lower percentages of plastic aggregates. This is evident from the steeper slopes between the age points for 0 % and 10 % plastic aggregates compared to 20 % and 30 % plastic aggregates. The positive effect of water curing on E_d compared to air curing is consistent with the general principles of concrete curing. This has been demonstrated in many previous studies [50].

The relative difference in E_d between different percentages of plastic aggregates becomes more pronounced with age, particularly for water-cured samples. This suggests that the negative impact of plastic aggregates on strength development becomes more significant over time. The incorporation of plastic masses reduces the dynamic modulus of elasticity of self-compacting concrete according to the obtained results, while water curing conditions with extended curing times help to improve and mitigate some of these negative effects. However, higher percentages of plastic masses (20 % and 30 %) still lead to significant reductions in E_d values.

3.3. Correlations

3.3.1. Correlation between the compressive strength and the ultrasonic pulse velocity and the water-to-cement ratio

The experimental results demonstrate a relationship between plastic aggregate content, compressive strength, ultrasonic pulse velocity, and water-to-cement ratio in the tested SCC. Fig. 20 illustrates these relationships for SCC without plastic aggregate (SCC_0) and with varying plastic aggregate content (SCC_{10}, SCC_{20}, and SCC_{30}) at 7, 28, 56, and 84-days. As the percentage of plastic aggregate increases from 0 % to 30 %, both C_S and UPV exhibit a non-linear, decreasing response across all sample ages. The parallel behavior of C_S and UPV curves implies a strong positive correlation between these properties, validating the efficacy of UPV as non-destructive testing method for strength assessment in this SCC. An attempt to model C_S as a function of UPV, and W/C ratio yielded an exponential relationship [50]:

$$C_S\,(\text{MPa}) = \alpha_1 \times EXP\,(\beta_1); \quad (6)$$

$$\alpha_1 = 17.132 \times (W/C) \text{ and } \beta_1 = 37.6\times V_{Ult}\,(\text{m/s}) \times 10^{-5}, \quad (7)$$

where α_1 and β_1 are regression coefficients of the exponential equation for each type of self-compacting concrete.

$$C_S(\text{MPa}) = 17.132\times(W/C)\times EXP\,(37.6\times V_{ult}(\text{m/s})\times 10^{-5}); \quad (8)$$

$$C_S(\text{MPa}) = 6.8528\times EXP(\,37.6\,V_{ult}(\text{m/s})\times 10^{-5}). \quad (9)$$

This model demonstrates a high correlation with experimental data (R^2 = 0.9781), providing a valuable tool for predicting compressive strength based on easily measurable parameters in SCC with varying plastic aggregate content.

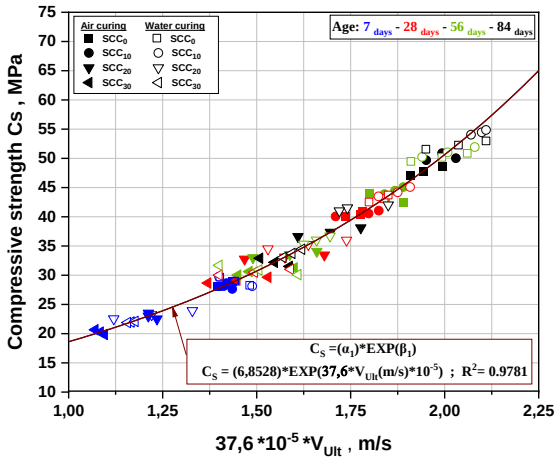

Fig. 20. Relationship between compressive strength and ultrasonic pulse velocity in self-compacting concrete with varying plastic aggregate content

Table 9 presents a comparative analysis between the experimentally measured compressive strength values (C_S measured) and those estimated (C_S estimated) using the Eq. 9. This comparison is made for SCC samples at various curing ages, considering both the ultrasonic pulse velocity and the water-to-cement ratio as key parameters. The relative error (%) calculated using Eq. 10, which compares the measured and estimated compressive strength values for the various experimental points of SCC, is generally less than 5 %.

$$\left|\frac{\Delta C_{S_i}}{C_{S_{i\,(Estimated)}}}\right| = \left|\frac{C_{S_{i\,(Estimated)}} - C_{S_{i\,(Measured)}}}{C_{S_{i\,(Estimated)}}}\right|. \quad (10)$$

This low error rate leads us to conclude that an accurate estimation of the compressive strength at different ages can be obtained by determining two key parameters: the ultrasonic pulse velocity V_{ult} and the W/C. This method provides a reliable non-destructive approach for assessing concrete strength development over time.

3.3.1. Correlation between the tensile strength and the ultrasonic pulse velocity

The experimental results demonstrate a relationship between plastic aggregate content, T_S, and UPV in the tested SCC. Fig. 21 illustrates these relationships for SCC without plastic aggregate (SCC_0) and with varying plastic aggregate content (SCC_{10}, SCC_{20}, and SCC_{30}) at 7, 28, 56, and 84-days. As the percentage of plastic aggregate increases from 0 % to 30 %, both T_S (MPa) and UPV (m/s) exhibit a non-linear decrease across all sample ages. The similar trends observed in T_S and UPV curves suggest a strong correlation between these properties, validating the efficacy of UPV as a non-destructive testing method for strength assessment in SCC.

Table 9. Experimental and estimated compressive strength values based on ultrasonic pulse velocity and water/cement ratio

Mixture	W/C	The calculations	The curing in air				The curing in water			
			Age, days							
			7	28	56	84	7	28	56	84
SCC_0	0.40	V_{ult}, m/s	3794.92	4721.04	4898.66	5167.95	3834.42	4891.03	5222.24	5403.67
		C_S estimated, MPa	28.55	40.44	43.23	47.84	28.97	43.11	48.82	52.27
		C_S measured, MPa	29.93	41.50	43.05	45.50	30.19	42.90	46.40	49.80
		Relative error, %	4.83	2.62	0.42	4.89	4.21	0.49	4.96	4.73
SCC_{10}	0.40	V_{ult}, m/s	3757.08	4728.47	4967.54	5300.65	3829.87	4963.35	5340.09	5512.44
		C_S estimated, MPa	28.14	40.55	44.37	50.28	28.92	44.30	51.04	54.45
		C_S measured, MPa	29.33	41.45	43.65	47.85	30.15	43.50	48.95	51.75
		Relative error, %	4.23	2.22	1.62	4.83	4.25	1.81	4.09	4.96
SCC_{20}	0.40	V_{ult}, m/s	3223.11	4188.45	4223.96	4510.44	3246.41	4355.53	4412.69	4790.98
		C_S estimated, MPa	23.02	33.10	33.54	37.36	23.23	35.25	36.01	41.52
		C_S measured, MPa	24.11	34.70	35.10	39.20	24.23	36.90	37.65	42.10
		Relative error, %	4.74	4.83	4.65	4.93	4.30	4.68	4.55	1.40
SCC_{30}	0.40	V_{ult}, m/s	2883.33	3850.16	3982.44	4115.18	3101.47	3972.74	4005.93	4239.30
		C_S estimated, MPa	20.26	29.15	30.63	32.20	21.99	30.52	30.90	33.74
		C_S measured, MPa	20.95	30.50	32.10	33.70	21.11	32.04	32.35	35.35
		Relative error, %	3.41	4.63	4.80	4.66	4.00	4.98	4.69	4.77

Modeling T_S as a function of UPV yielded an exponential relationship:

$$T_S\ (\text{MPa}) = \alpha_2 \times (V_{Ult}\ (\text{m/s}))^{(\beta 2)}; \quad (11)$$

$$\alpha_2 = 12.725 \times 10^{-9} \text{ and } \beta_2 = 2.3186, \quad (12)$$

where α_2 and β_2 are regression coefficients of the exponential equation for each type of self-compacting concrete.

$$T_S\ (\text{MPa}) = 12.725 \times 10^{-9} \times (V_{Ult}\ (\text{m/s}))^{2.3186}. \quad (13)$$

This model demonstrates a high correlation with experimental data (R^2 = 0.9737), providing a valuable tool for predicting tensile strength based on easily measurable parameters in SCC with varying plastic aggregate content.

Table 10 presents a comparative analysis between the experimentally measured tensile strength values (T_S measured) and those estimated (T_S estimated) using Eq. 13. This comparison is made for SCC samples at various curing ages, considering V_{ult} as key parameters.

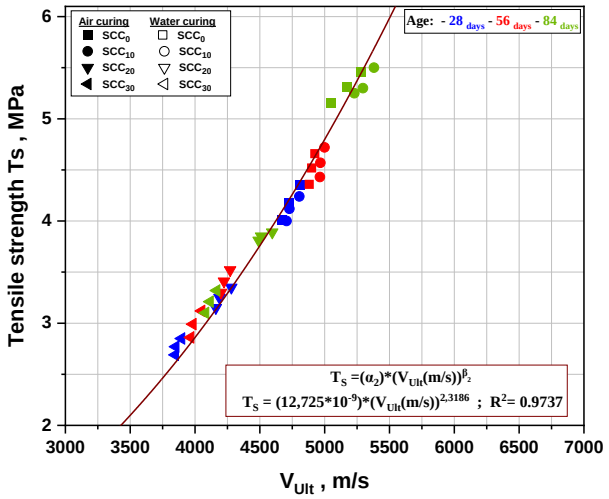

Fig. 21. Relationship between tensile strength and ultrasonic pulse velocity in self-compacting concrete with varying plastic aggregate content

Table 10. Experimental and estimated tensile strength values based on ultrasonic pulse velocity

Mixture	The calculations	The curing in air			The curing in water		
		Age, days					
		28	56	84	28	56	84
SCC_0	V_{ult}, m/s	4721.04	4898.66	5167.95	4891.03	5222.24	5403.67
	T_S estimated, MPa	4.20	4.58	5.18	43.11	48.82	52.27
	T_S measured, MPa	4.18	4.52	5.31	42.90	46.40	49.8
	Relative error, %	0.47	1.31	2.51	4.82	6.91	2.79
SCC_{10}	V_{ult}, m/s	4728.47	4967.54	5300.65	4963.35	5340.09	5512.44
	T_S estimated, MPa	4.22	4.73	5.49	4.72	5.59	6.02
	T_S measured, MPa	4.12	4.57	5.35	4.44	4.97	5.69
	Relative error, %	2.37	3.38	2.55	5.93	6.09	5.48
SCC_{20}	V_{ult}, m/s	4188.45	4223.96	4510.44	4355.53	4412.69	4790.98
	T_S estimated, MPa	3.18	3.25	3.78	3.48	3.59	4.35
	T_S measured, MPa	3.25	3.41	3.85	3.33	3.68	4.15
	Relative error, %	2.20	4.92	1.85	4.31	2.51	4.60
SCC_{30}	V_{ult}, m/s	3850.16	3982.44	4115.18	3972.74	4005.93	4239.30
	T_S estimated, MPa	2.62	2.83	3.05	2.82	2.87	3.27
	T_S measured, MPa	2.77	2.99	3.21	2.95	3.04	3.42
	Relative error, %	5.73	5.65	5.25	4.61	5.92	4.59

The relative error (%) calculated using Eq. 14, which compares the measured and estimated tensile strength values for the various experimental points of SCC, is generally less than 7 %. This low error rate leads us to conclude that an accurate estimation of the tensile strength at different ages can be obtained by determining the ultrasonic pulse velocity V_{ult}. This method provides a reliable non-destructive approach for assessing concrete strength development over time.

$$\left|\frac{\Delta T_{S_i}}{T_{S_i\,(Estimated)}}\right| = \left|\frac{T_{S_i\,(Estimated)} - T_{S_i\,(Measured)}}{T_{S_i\,(Estimated)}}\right|. \quad (14)$$

4. CONCLUSIONS

In this experimental investigation, we examined the physical-mechanical and rheological characteristics of self-compacting concrete mixes with varying percentages of plastic aggregate in both their fresh and hardened phases. The results of this experimental work demonstrate the benefits of using plastic aggregate instead of natural aggregate to create SCC that is both environmentally friendly. Based on the experimental program and modeling results, we can draw the following key conclusions:

1. The use of plastic aggregate instead of natural aggregate generally improved the flowability and passing ability of SCC, as evidenced by increased slump flow and J-ring flow values, as well as decreased T_{500} and V-funnel times (T_V), and in addition, the height of the L-box. When substitution levels greater than 30 % are used, the separation resistance decreases.
2. As the percentage of plastic aggregates increases relative to natural aggregates, the density of SCC decreases, which can be beneficial for lightweight applications. At the same time, it results in higher water absorption and increased porosity.
3. There is a noticeable decline in both compressive and tensile strengths with higher plastic content, particularly beyond a 10 % replacement level. While SCC with up to 10 % plastic aggregate (SCC_{10}) maintains comparable performance to control SCC (SCC_0).
4. Replacing natural aggregate with higher levels of plastic aggregate results in significant reductions in ultrasonic pulse velocity and dynamic modulus of elasticity.
5. A 10 % replacement level is the optimum level to maintain a balance between acceptable performance and the benefits of using recycled plastic. Adding 20 % plastic aggregate to SCC cured with water for 84-days improves its compressive strength and UPV compared to the reference SCC (SCC_0) cured with air for 28-days.
6. Tests on self-compacting concrete without and with plastic aggregates showed a strong correlation between destructive (compressive strength, *C*s) and non-destructive (ultrasonic pulse velocity, V_{ult}). Compared to measured values, the estimated compressive strength based on this correlation had a relative error of less than 5 %. This result provides practical tools for quality control and performance prediction in SCC with alternative aggregates, such as plastic.
7. The curing in water has a beneficial effect on reducing the porosity of all self-compacting concrete, as well as increasing the tensile strength, compressive strength, and ultrasonic pulse velocity.
8. A critical contribution of this research is the identification of optimization thresholds for different applications. For structural applications, plastic aggregate content should not exceed 10 % to maintain optimal mechanical properties. However, non-structural applications can accommodate up to 20 % plastic aggregate content, while architectural applications may utilize up to 30% replacement levels when appropriate curing conditions are maintained.
9. Looking forward, this research opens several promising avenues for future investigation. Priority areas include long-term durability assessment beyond 84-days, compatibility studies with different types of plastic waste, and development of surface treatment methods for plastic aggregates. Additionally, research into chemical interactions between plastic and cement hydration products could lead to improved mix designs and performance enhancement strategies.

Finally, the incorporation of plastic aggregates in elf-compacting concrete represents a viable strategy for recycling plastic waste and reducing the environmental impact of concrete production. This study provides valuable insights into the material properties over time, with significant implications for sustainable construction practices and the utilization of waste plastic in building materials.

REFERENCES

1. **Okamura, H., Ouchi, M.** Self-Compacting Concrete *Journal of Advanced Concrete Technology* 1 (1) 2003: pp. 5 – 15. https://doi.org/10.3151/jact.1.5
2. **Meko, B., Ighalo, J.O., Ofuyatan, O.M**. Enhancement of Self-Compactability of Fresh Self-Compacting Concrete: A Review *Cleaner Materials* 1 2021: pp. 100019. https://doi.org/10.1016/j.clema.2021.100019
3. **Al-Shetwi, A.Q.** Sustainable Development of Renewable Energy Integrated Power Sector: Trends, Environmental Impacts, and Recent Challenges *The Science of the Total Environment* 822 2022: pp. 153645. https://doi.org/10.1016/j.scitotenv.2022.153645
4. **Sandanayake, M., Zhang, G., Setunge, S.** Estimation of Environmental Emissions and Impacts of Building Construction – A Decision-Making Tool for Contractors *Journal of Building Engineering* 21 2019: pp. 173 – 85. https://doi.org/10.1016/j.jobe.2018.10.023
5. **Yang, M., Chen, L., Wang, J., Msigwa, G., Osman, A.I., Fawzy, S., Yap, P.** Circular Economy Strategies for Combating Climate Change and other Environmental Issues *Environmental Chemistry Letters* 21 (1) 2022: pp. 55 – 80. https://doi.org/10.1007/s10311-022-01499-6
6. **Hamada, H.M., Al-Attar, A., Abed, F., Beddu, S., Humada, A.M., Majdi, A., Thomas, B.S.** Enhancing Sustainability in Concrete Construction: A Comprehensive Review of Plastic Waste as an Aggregate Material *Sustainable Materials and Technologies* 40 2024: pp. e00877. https://doi.org/10.1016/j.susmat.2024.e00877

7. **Aldahdooh, M.A.A., Jamrah, A., Alnuaimi, A., Martini, M.I., Ahmed, M.S.R., Ahmed, A.S.R.** Influence of Various Plastics-Waste Aggregates on Properties of Normal Concrete *Journal of Building Engineering* 17 2018: pp. 13 – 22. https://doi.org/10.1016/j.jobe.2018.01.014
8. **Nematzadeh, M., Mousavimehr, M.** Residual Compressive Stress–Strain Relationship for Hybrid Recycled PET–Crumb Rubber Aggregate Concrete after Exposure to Elevated Temperatures *Journal of Materials in Civil Engineering* 31 (8) 2019: pp. 04019136. https://doi.org/10.1061/(asce)mt.1943-5533.0002749
9. **Gautam, B.P.S., Qureshi, A., Gwasikoti, A., Kumar, V., Gondwal, M.** Global Scenario of Plastic Production, Consumption, and Waste Generation and their Impacts on Environment and Human Health *In Advanced Strategies for Biodegradation of Plastic Polymers. Cham: Springer Nature Switzerland* 2024: pp. 1 – 34. https://doi.org/10.1007/978-3-031-55661-6_1
10. **Tiwari, R., Azad, N., Dutta, D., Yadav, B.R., Kumar, S.** A Critical Review and Future Perspective of Plastic Waste Recycling *The Science of the Total Environment* 881 2023: pp. 163433. https://doi.org/10.1016/j.scitotenv.2023.163433
11. **Almeshal, I., Tayeh, B.A., Alyousef, R., Alabduljabbar, H., Mohamed, A.M., Alaskar, A.** Use of Recycled Plastic as Fine Aggregate in Cementitious Composites: A Review *Construction and Building Materials* 253 2020: pp. 119146. https://doi.org/10.1016/j.conbuildmat.2020.119146
12. **Awoyera, P.O., Adesina, A.** Plastic Wastes to Construction Products: Status, Limitations and Future Perspective *Case Studies in Construction Materials* 12 2020: pp. e00330. https://doi.org/10.1016/j.cscm.2020.e00330
13. **Gu, L., Ozbakkaloglu, T.** Use of recycled Plastics in Concrete: A Critical Review *Waste Management* 51 2016: pp. 19 – 42. https://doi.org/10.1016/j.wasman.2016.03.005
14. **Saikia, N., De Brito, J.** Use of Plastic Waste as Aggregate in Cement Mortar and Concrete Preparation: A Review *Construction and Building Materials* 34 2012: pp. 385 – 401. https://doi.org/10.1016/j.conbuildmat.2012.02.066
15. **Zulkernain, N.H., Gani, P., Chuan, N.C., Uvarajan, T.** Utilisation of Plastic Waste as Aggregate in Construction Materials: A Review *Construction and Building Materials* 296 2021: pp. 123669. https://doi.org/10.1016/j.conbuildmat.2021.123669
16. **Babafemi, A., Šavija, B., Paul, S., Anggraini, V.** Engineering Properties of Concrete with Waste Recycled Plastic: A Review *Sustainability* 10 (11) 2018: pp. 3875. https://doi.org/10.3390/su10113875
17. **Mercante, I., Alejandrino, C., Ojeda, J.P., Chini, J., Maroto, C., Fajardo, N.** Mortar and Concrete Composites with Recycled Plastic: A Review *Science and Technology of Materials* 30 2018: pp. 69 – 79. https://doi.org/10.1016/j.stmat.2018.11.003
18. **Chunchu, B.R.K., Putta, J.** Effect of Recycled Plastic Granules as a Partial Substitute for Natural Resource Sand on the Durability of SCC *Resources* 8 (3) 2019: pp. 133. https://doi.org/10.3390/resources8030133
19. **Shobeiri, V., Bennett, B., Xie, T., Visintin, P.** Mix Design Optimization of Waste-based Aggregate Concrete for Natural Resource Utilization and Global Warming Potential *Journal of Cleaner Production* 449 2024: pp. 141756. https://doi.org/10.1016/j.jclepro.2024.141756
20. **Li, X., Ling, T.C., Mo, K.H.** Functions and Impacts of Plastic/Rubber Wastes as Eco-Friendly Aggregate in Concrete – A Review *Construction and Building Materials* 240 2020: pp. 117869. https://doi.org/10.1016/j.conbuildmat.2019.117869
21. **Houcine, B., Mohamed, R., Samir, K., Sarra, B.** Valorization of Plastic Waste in Concrete for Sustainable Development *The Journal of Engineering and Exact Sciences* 9 (5) 2023: pp. 16009–01e. https://doi.org/10.18540/jcecvl9iss5pp16009-01e
22. **Al-Mansour, A., Zhu, Y., Lan, Y., Dang, N., Alwathaf, A.H., Zeng, Q.** Improving the Adhesion Between Recycled Plastic Aggregates and the Cement Matrix. In: Elsevier eBooks. 2024: pp. 113 – 138. https://doi.org/10.1016/b978-0-443-13798-3.00008-5
23. **Alkhrissat, T.** Impact of Adding Waste Polyethylene (PE) and Silica Fume (SF) on the Engineering Properties of Cement Mortar *Case Studies in Chemical and Environmental Engineering* 9 2024: pp. 100731. https://doi.org/10.1016/j.cscee.2024.100731
24. **Sau, D., Shiuly, A., Hazra, T.** Utilization of Plastic Waste as Replacement of Natural Aggregates in Sustainable Concrete: Effects on Mechanical and Durability Properties *International Journal of Environmental Science and Technology* 21 (2) 2023: pp. 2085 – 2120. https://doi.org/10.1007/s13762-023-04946-1
25. **ASTM.** International. Standard Specification for Lightweight Aggregates for Structural Concrete (ASTM C330/C330M - 09). ASTM International, West Conshohocken, Pennsylvania, 2009. https://doi.org/10.1520/C0330
26. **ACI.** Committee E- 701. Aggregates for concrete (ACI E1 07). American Concrete Institute; 2007. https://doi.org/10.1201/9781315272436-20
27. **Rachid, R., Mohamed, A., Mohamed, R., Mohammed, O.** Effect of Additions on The Self-Compacting Concrete's Absorption *The Journal of Engineering and Exact Sciences* 9 (6) 2023: pp. 16058–01e. https://doi.org/10.18540/jcecvl9iss6pp16058-01e
28. **Su, N., Miao, B.** A New Method for the Mix Design of Medium Strength flowing Concrete with Low Cement Content *Cement and Concrete Composites* 25 (2) 2003: pp. 215 – 222. https://doi.org/10.1016/s0958-9465(02)00013-6
29. **Brouwers, H.J.H., Radix, H.J.** Self-Compacting Concrete: Theoretical and Experimental Study *Cement and Concrete Research* 35 (11) 2005: pp. 2116 – 2136. https://doi.org/10.1016/j.cemconres.2005.06.002
30. **BIBM.** The European Project Group, The European Guidelines for Self- Compacting Concrete: Specification, Production and Use 563 2005: pp. 22. http://www.efnarc.org/pdf/SCCGuidelinesMa y2005.pdf
31. **Yang, L., Liu, G., Gao, D., Zhang, C.** Experimental Study on Water Absorption of Unsaturated Concrete: W/C Ratio, Coarse Aggregate and Saturation Degree *Construction and Building Materials* 272 2021: pp. 121945. https://doi.org/10.1016/j.conbuildmat.2020.121945
32. **Zhuang, S., Wang, Q., Zhang, M.** Water Absorption Behaviour of Concrete: Novel Experimental Findings and Model Characterization *Journal of Building Engineering* 53 2022: pp. 104602. https://doi.org/10.1016/j.jobe.2022.104602

33. **ASTM C597–02.** Standard Test Method for Pulse Velocity Through Concrete. Annual Book of ASTM Standards, Vol. 04, Philadelphia, 2002.
34. **Hobbs, B., Kebir, M.T.** Non-Destructive Testing Techniques for the Forensic Engineering Investigation of Reinforced Concrete Buildings *Forensic Science International* 167 (2 – 3) 2007: pp. 167 – 172. https://doi.org/10.1016/j.forsciint.2006.06.065
35. **Gupta, T., Chaudhary, S., Sharma, R.K.** Mechanical and Durability Properties of Waste Rubber Fiber Concrete with and without Silica Fume *Journal of Cleaner Production* 112 2016: pp. 702 – 711. https://doi.org/10.1016/j.jclepro.2015.07.081
36. **Aswatama, W.K., Suyoso, H., Meyfa, U.N., Tedy, P.** The Effect of Adding PET (Polyethylen Terephthalate) Plastic Waste on SCC (Self-Compacting Concrete) to Fresh Concrete Behavior and Mechanical Characteristics *Journal of Physics Conference Series* 953 (1) 2018: p. 012023. https://doi.org/10.1088/1742-6596/953/1/012023
37. **Faraj, R.H., Ali, H.F.H., Sherwani, A.F.H., Hassan, B.R., Karim, H.** Use of Recycled Plastic in Self-Compacting Concrete: A Comprehensive Review on Fresh and Mechanical Properties *Journal of Building Engineering* 30 2020: pp. 101283. https://doi.org/10.1016/j.jobe.2020.101283
38. **Hama, S.M., Hilal, N.N.** Fresh Properties of Self-Compacting Concrete with Plastic Waste as Partial Replacement of Sand *International Journal of Sustainable Built Environment* 6 (2) 2017: pp. 299 – 308. https://doi.org/10.1016/j.ijsbe.2017.01.001
39. **Safi, B., Saidi, M., Aboutaleb, D., Maallem, M.** The Use of Plastic Waste as Fine Aggregate in the Self-Compacting Mortars: Effect on Physical and Mechanical Properties *Construction and Building Materials* 43 2013: pp. 436 – 442. https://doi.org/10.1016/j.conbuildmat.2013.02.049
40. **Sau, D., Shiuly, A., Hazra, T.** Utilization of Plastic Waste as Replacement of Natural Aggregates in Sustainable Concrete: Effects on Mechanical and Durability Properties *International Journal of Environmental Science and Technology* 21 2024: pp. 2085 – 2120. https://doi.org/10.1007/s13762-023-04946-1
41. **Mohammed, H., Sadique, M., Shaw, A., Bras, A.** The Influence of Incorporating Plastic Within Concrete and the Potential use of Microwave Curing; A Review *Journal of Building Engineering* 32 2020: pp. 101824. https://doi.org/10.1016/j.jobe.2020.101824
42. **Korouzhdeh, T., Eskandari-Naddaf, H., Kazemi, R.** The ITZ Microstructure, Thickness, Porosity and its Relation with Compressive and Flexural Strength of Cement Mortar; Influence of Cement Fineness and Water/Cement Ratio *Frontiers of Structural and Civil Engineering* 16 2022: pp. 191 – 201. https://doi.org/10.1007/s11709-021-0792-y
43. **Alanazi, H.** Study of the Interfacial Transition Zone Characteristics of Geopolymer and Conventional Concretes *Gels* 8 (2) 2022: pp. 105. https://doi.org/10.3390/gels8020105
44. **Sharma, M., Bishnoi, S.** The Interfacial Transition Zone: Microstructure, Properties, and Its Modification. In: Rao, A., Ramanjaneyulu, K. (eds) Recent Advances in Structural Engineering, Volume 2. Lecture Notes in Civil Engineering, vol 12, 2019. Springer, Singapore. https://doi.org/10.1007/978-981-13-0365-4_63
45. **Sharma, R., Bansal, P.P.** Use of Different Forms of Waste Plastic in Concrete – A Review *Journal of Cleaner Production* 112 2016: pp. 473 – 482. https://doi.org/10.1016/j.jclepro.2015.08.042
46. **Saikia, N., De Brito, J.** Mechanical Properties and Abrasion Behaviour of Concrete Containing Shredded PET Bottle Waste as a Partial Substitution of Natural Aggregate *Construction and Building Materials* 52 2014: pp. 236 – 244. https://doi.org/10.1016/j.conbuildmat.2013.11.049
47. **Sadrmomtazi, A., Dolati-Milehsara, S., Lotfi-Omran, O., Sadeghi-Nik, A.** The Combined Effects of Waste Polyethylene Terephthalate (PET) Particles and Pozzolanic Materials on the Properties of Self-Compacting Concrete *Journal of Cleaner Production* 112 2016: pp. 2363 – 2373. https://doi.org/10.1016/j.jclepro.2015.09.107
48. **Jaskowska-Lemańska, J., Kucharska, M., Matuszak, J., Nowak, P., Łukaszczyk, W.** Selected Properties of Self-Compacting Concrete with Recycled PET Aggregate *Materials* 15 (7) 2022: pp. 2566. https://doi.org/10.3390/ma15072566
49. **Gu, L., Ozbakkaloglu, T.** Use of Recycled Plastics in Concrete: A Critical Review *Waste Management* 51 2016: pp. 19 – 42. https://doi.org/10.1016/j.wasman.2016.03.005
50. **Rabehi, R., Rabehi, M., Omrane, M.** Physical-mechanical and Fresh State Properties of Self-Compacting Concrete Based on Different Types of Gravel Reinforced with Steel Fibers: Experimental Study and Modeling *Construction and Building Materials* 390 2023: pp. 131758. https://doi.org/10.1016/j.conbuildmat.2023.131758